Soluble (pro)renin receptor promotes fibrotic response in renal proximal tubule epithelial cells in vitro via Akt/β-catenin/Snail signaling pathway

Authors

Shiying Xie [1, 2], Jiahui Su [1], Aihua Lu [1], Ying Lai [1], Shiqi Mo [1], Min Pu [1], Tianxin Yang [1, 2, 3]

1 Institute of Hypertension, Zhongshan School of Medicine, Sun Yat-sen University, Guangzhou, China.

2 Department of Internal Medicine, University of Utah and Veterans Affairs Medical Center, Salt Lake City, Utah, USA.

3 The First Affiliated Hospital of Zhengzhou University, Zhengzhou, China.

Corresponding Author

Tianxin Yang, M.D., Ph.D.

Division of Nephrology and Hypertension

University of Utah and Veterans Affairs Medical Center

30N 1900E, RM 4R214

Salt Lake City, UT 84132

Email: Tianxin.Yang@hsc.utah.edu

Tel: 801-585-5570

Abstract

Tubulointerstitial fibrosis has been regarded as a critical event in the pathogenesis of chronic kidney disease (CKD). Soluble form of PRR (sPRR), generated by site-1 protease (S1P) cleavage of full-length PRR, is detected in biological fluid and elevated under certain pathological conditions. The present study was designed to evaluate the potential role of sPRR in regulation of fibrotic response in cultured human renal proximal tubular cell line human kidney 2 (HK-2) cells, in the setting of TGF-β or sPRR-His treatment. TGF-β induced fibrotic response of HK-2 cells was indicated by the upregulation of fibronectin (FN) expression, meanwhile, TGF-β could also induce the generation of sPRR, due to enhanced cleavage of fPRR. To explore the role of sPRR in fibrotic response of HK-2 cells, we blocked the production of sPRR with a S1P inhibitor PF429242 and found that PF429242 remarkably suppressed TGF-β induced sPRR generation and FN expression in HK-2 cells. Administration of sPRR-His restored PF429242 attenuated FN expression in HK-2 cells, indicating that sPRR could promote TGF-β induced fibrotic response. Furthermore, sPRR-His alone also increased the abundance of FN in HK-2 cells. These data suggested that sPRR was sufficient and necessary for TGF-ß-induced fibrotic response of HK-2 cells. Mechanistically, sPRR activated the AKT and β-catenin pathway in HK-2 cells, and blockade of AKT or β-catenin pathway significantly abrogated sPRR-induced FN and Snail expression. Taking together, sPRR promoted the fibrotic response of HK-2 cells by activating Akt/β-catenin/Snail signaling, and it may serve as a potential therapeutic target in renal fibrosis.

Introduction

Tubulointerstitial fibrosis (TIF) is a reliable predictor of prognosis and a major determinant of renal insufficiency and it is also a chronic and progressive process affecting kidneys during aging and in CKD(13, 21). TIF is a common irreversible process characterized by replacement of cellular parenchyma and progressive loss of renal function, uncontrolled deposits of extracellular matrix protein (37). Activation of fibroblasts and myofibroblasts are largely responsible for excessive matrix synthesis and tissue deposition (34). The activation is initiated by many profibrotic molecules, including transforming growth factor-β (TGF-β); connective tissue growth factor (CTGF); platelet-derived growth factor; interleukin (IL)-4, IL-6, and IL-13; and endothelin-1(13, 21, 25).

TGF-β is generally considered as a central mediator of fibrotic diseases(36). Inhibition of the TGF-β isoform, TGF-β1, or its downstream signaling pathways substantially limits renal fibrosis in a wide range of disease models(2, 26, 35) , whereas overexpression of TGF-β induces renal fibrosis(22). As known, TGF-β induces renal fibrosis via activation of both canonical (Smad-based) and non-canonical (non-Smad-based) signaling pathways, including MAPKs, the TGF-β activated kinase 1 (TAK1) pathway, phosphatidylinositol 3-kinase (PI3K)/AKT and integrin-linked kinase (ILK), which results in activation of myofibroblasts, excessive production of extracellular matrix (ECM) and inhibition of ECM degradation(1, 15, 19).

In 2002, Nguyen and co-workers reported the expression of a specific binding receptor, named (pro)renin receptor (PRR), and identified the catalytic function after binding renin and prorenin (30). The full-length PRR (fPRR) is a unique 350-amino-acid transmembrane protein, which contains the furin and site-1 protease (S1P) cleavage sites. Cleaved by furin or S1P, fPRR was generated to a 28-kDa N-terminal region, soluble PRR (sPRR), and a C-terminal

transmembrane form (M8.9 complexed with V-ATPase) (4, 7, 27). Despite the effects of fPRR in hypertension (17, 18, 31), kidney disease (20, 29), pre-eclampsia (28), cardiovascular disease (6, 24) were widely studied, the function of sPRR was rarely focused. The emerging evidence showed the physiological and pathological function of sPRR, in regulation of renal water balance (23), systemic renin-angiotensin system(8, 33) and blood pressure (9). Therefore, the present study was intended to study a biological function and signaling of sPRR in the regulation of fibrotic response in HK-2 cells.

Materials and Methods

Materials

Dulbecco's modified Eagle's medium/nutrient mixture F1-2 (DMEM/F-12) purchased from Life Technologies (Grand Island, NY, USA). Fetal bovine serum was purchased from Quacell Biotechnology (Zhongshan, Guangdong, China). TGF-β was purchased from Sino Biological (Beijing, China). PF-429242 was purchased from AdooQ Biosciences (Irvine, CA, USA). LY 294002, ICG-001 and losartan were purchased from Medchemexpress (Stockholm, Sweden). sPRR-His was generated by Xbio (Shanghai, CN).

Cell culture

The human renal proximal tubular epithelial cell line (HK-2) was from normal male adult kidney and immortalized by transduction with human papilloma virus 16/E6/E7 genes. HK-2 cells were obtained from Procell Life Science Co., Ltd. Cells were cultured in DMEM/F-12, containing 10% fetal bovine serum (FBS) and 1% penicillin/streptomycin at 37°C under 5% CO2 in a humidified incubator. For all experiments, cells were grown on 6-well plates to reach 80%-90% confluence and serum starvation was established for 12 hours with DMEM/F12

medium that contained no drugs or hormones before treatment. Microscopic examination was performed during indicated experiment to assess the morphological changes.

ELISA measurement of sPRR

Cell culture medium was collected at the end of treatments and the concentration of sPRR in cell culture medium was determined by using sPRR ELISA kit (Immuno-Biological Laboratories, Takasaki, Japan). Followed the instruction of the kit, for each sample, 100 microliter cell medium and diluted standards was added to the corresponding well. After incubating at 4℃ overnight, the wells were washed four times with wash buffer and 100 μl of antibody solution was pipetted into the wells. The elisa plate was incubated at 4℃ for 60 min and the wash step repeated. Chromogen was added into each washed well and incubated for 30min at room temperature in dark. The stop buffer was intended to end the reaction in each well, after mixing completely with chromogen, the OD value was ready to be detect.

Immunoblotting

Cells were lysed and subsequently sonicated in RIPA buffer mixed with cocktail. After centrifugation, the protein concentration was determined by the Pierc BCA Protein Assay Kit (Thermo Scientific, Rockford, IL, USA). Twenty micrograms of protein from whole cell lysate was separated by SDS-polyacrylamide gel electrophoresis and transferred onto 0.22 μm polyvinylidene fluoride membranes (Amersham Pharmacia Biotech, Piscataway, NJ, USA). The blots were blocked in 5% skim milk in Tris-buffered saline with Tween-20 (TBST) at room temperature for 1h, followed by incubation with rabbit anti-PRR antibody, anti-FN antibody, anti-p-AKT (Thr308) antibody, anti-p-AKT (Ser473) antibody, anti-AKT antibody, anti-β-catenin antibody, anti-Snail antibody or mouse monoclonal anti-β-GAPDH antibody at 4℃. After washing three times with TBST, blots were incubated with secondary antibody (goat

anti-rabbit/mouse horseradish peroxidase (HRP) - conjugated secondary antibody), followed by three times washing. Antibody labeling was visualized by addition of chemiluminescence substrate for detection of HRP.

Nuclear and Cytoplasmic Fractionation

Nuclear and cytoplasmic lysates were obtained by using the Nuclear and Cytoplasmic Extraction Kit (KeyGEN BioTECH) according to the manufacturer's instruction for Western blotting assay.

RNA isolation and qRT-PCR

Total RNA was extracted using TRIzol Reagent (Invitrogen) according to the manufacturer's instruction. Total RNA (500 ng) was reverse transcribed into cDNA using the cDNA synthesis kit (Takara Bio, Shiga, Japan) and qRT–PCR was carried out using real-time PCR system (Applied Biosystems). GAPDH was detected as an internal control. Primer sequences were designed by OriGene Technologies (available at https://www.origene.com/category/gene-expression/qpcr-primer-pairs).

Immunofluorescence Analysis

HK-2 cells were grown on coated glass coverslips for defined periods of time. After the treatment, HK-2 cells were washed with PBS for 3 times, then fixed for 10 minutes in 4% paraformaldehyde/PBS. The fixed cells were washed and then permeabilized for 15 minutes at room temperature with PBS containing 0.1% Triton X-100, then blocked with PBS including 5% BSA and incubated overnight at 4°C with primary anti-FN (1:200) antibody diluted 1% BSA/PBS. The next day, sections were washed and incubated for 1 hour at room temperature with secondary antibodies (Invitrogen), then embedded in Vectorshield mounting

medium with DAPI (Vector Laboratories).

Data Analysis

All data in text and figures are provided as means ± SEM. The results analysis was performed by using a one-way Analysis of Variance (ANOVA) or Tukey's post-hoc test. GraphPad Prism 6 software was used for statistical analyses. A p value of <0.05 was considered statistically significant.

Result

TGF-β induced fibrotic response and generation of sPRR

Fibrotic response and generation of sPRR was induced by exposure of HK-2 cells to TGF-β at 10 g/ml for 24h, as reflected by immunoblotting detection of increased FN and sPRR protein abundance, while the fPRR expression was unchanged under the stimulation (Fig. 1A). Consistent with the immunoblotting analysis, the released sPRR in cell culture medium was also induced by TGF-β (Fig. 1B). And in the mRNA levels, FN expression was significantly stimulated by TGF-β (Fig. 1C). As a well-characterized inducer of EMT in HK-2 cells, TGF-β treatment promoted a conversion to spindle-like morphology, whereas the control group exhibit typical epithelial-like morphology (Fig. 1D). We next detected the deposition of FN on HK-2 cells by using immunofluorescence. The results showed enhanced FN labeling after TGF-β treatment (Fig. 1E).

sPRR contributes to TGF-β-induced fibrotic response

Due to the increased generation of sPRR, we turned our attention on the potential role of sPRR on TGF-β induced fibrotic response. To investigate the involvement of sPRR, we used 40μM S1P inhibitor PF429242 to block the cleavage of PRR. As expected, upon the inhibition of the sPRR generation, the induced FN was completely suppressed by treating with PF429242 (Fig. 2A). Furthermore, the increased medium sPRR was completely abolished by PF429242 treatment (Fig. 2B). To identify the signaling pathway(s) that sPRR might activate the fibrotic response of HK-2 cells, the signaling proteins were detected. We firstly detected the role of AKT since TGF-β was demonstrated to be able to induce fibrotic response in HK-2 cells by activating AKT(10, 43). Phosphorylated AKT was significantly induced by treatment of TGF-β at 15 min, which was blocked by PF429242, indicating the involvement of AKT in sPRRmediated fibrotic response (Fig. 2C). As a pivotal fibrotic

regulator, β-catenin was activated under the TGF-β stimulation, and acted as a downstream element of AKT participating in the epithelial cell fibrotic response(5, 10, 41). To explore the involvement of β-catenin in the fibrotic response, we examined the translocation of β-catenin in TGF-β stimulated HK-2 cell after PF429242 treatment. PF429242 significantly suppressed the TGF-β induced nuclear β-catenin translocation, companied with increased cytosolic β-catenin abundance (Fig. 2D&E). As a potential downstream transcription regulator of β-catenin, the Snail expression was determined. Result showed the striking inhibitory effect of PF429242 on the TGF-β induced Snail expression (Fig. 2F). Furthermore, PF429242 suppressed the TGF-β increased mRNA levels of FN, Snail and S1P (Fig. 2G). We also tested the effect of PF429242 on TGF-β induced EMT. As expected, PF429242 blocked the TGF-β induced EMT (Fig. 2H). Immunostaining was conducted to confirm the effect of PF429242 on FN protein abundance. Upon the treatment of PF429242, TGF -β stimulated FN expression was obviously suppressed (Fig.2I).

In order to further validate the role of sPRR in TGF-β induced fibrotic response, the reversibility of sPRR-His on PF429242 reduced fibrotic response was tested. As expected, 60 nM sPRR-His restored the PF429242 reduced FN protein abundance which was stimulated by TGF-β for 24h (Fig. 3A). The addition of sPRR-His in cell culture medium also increased the sPRR concentration in TGF-β + PF429242 group (Fig. 3B). On the mechanism, p-AKT was significantly increased after 15 min stimulation with TGF-β and this response was blocked by PF429242 which was reversed by supplement of sPRR-His (Fig. 3C). The PF429242 abolished abundance of nuclear β-catenin was modestly restored by sPRR-His (Fig. 3D), companied by the decreased cytosolic β-catenin content (Fig. 3E). The inhibitory effect of PF429242 on TGF-β-induced Snail protein expression was also reversed by sPRR-His (Fig. 3F). At the mRNA levels, qRT-PCR detected parallel increases in mRNA expression of FN

and Snail in TGF-β stimulated HK-2 cells, which were both suppressed by PF-429242 and partially reversed by sPRR-His (Fig. 3G). However, the administration of sPRR-His showed no effect on the cell morphology (Fig. 3H). The immunostaining further validated the effect of sPRR-His and PF429242 on TGF-β stimulated FN deposition (Fig. 3I).

Taken together, the results presented above indicated that sPRR contributes to fibrotic response via AKT/β-catenin/Snail signaling pathway in TGF-β stimulated HK-2 cells.

sPRR-His induced fibrotic response in HK-2 cells

To explore the direct effect of sPRR on fibrotic response, HK-2 cells were treated with sPRR-His, and the expression of FN were evaluated by immunoblotting. As expected, sPRR-His induced an obvious increase of the FN, companied with upregulated AKT phosphorylation and Snail expression (Fig. 4A). Consisting with the protein expression, the mRNA levels of FN and Snail were also increased (Fig. 4B). To explore the effect of sPRR-His on EMT, we determined the expression of α-SMA, collagen I and E-cadherin and analyzed the cell morphology. sPRR-His increased the expression of α-SMA and collagen I, but showed no effect on E-cadherin expression or cell morphology (Fig. 4 C&D). By immunofluorescence, FN protein deposition was also significantly induced by sPRR-His treatment (Fig. 4E). These results suggested that the indicated treatment of sPRR-His could directly stimulate the fibrotic response but may not be sufficient to drive EMT in HK-2 cells.

sPRR-His promoted fibrotic response depending on AT1 receptor mediated endocytosis

Given the potential association between PRR/sPRR and the RAS, we tested the dependence of sPRR-His induced fibrotic response on the AT1 receptor. Losartan remarkably decreased cytosolic sPRR-His concentration and sPRR-His stimulated FN protein expression, AKT phosphorylation and Snail protein expression in HK-2 cells (Fig. 5A). The

sPRR-His-induced mRNA expression of FN and Snail were also blocked by losartan treatment (Fig. 5B). We further examined the FN by immunostaining, consistent with the Western blot results, losartan blocked sPRR-His-induced FN expression (Fig. 5C). The results demonstrated that sPRR-His induced fibrotic response relied on the AT1 receptor.

sPRR-His contributed to fibrotic response via AKT/β-catenin/Snail signaling pathway.

To identify the signaling pathway(s) contributing to sPRR-His induced fibrotic response, we examined the AKT/β-catenin/Snail pathway. Immunoblotting analysis showed the inhibitory effect of 10μM LY294002 (a PI3K inhibitor) on the phosphorylation levels of AKT. As expected, this inhibitor successfully reduced the phosphorylation level of the AKT proteins, paralleled by the completely inhibition of FN and Snail protein abundance and mRNA expression (Fig. 6A&B). Above observation was associated with the suppressed FN expression detected by immunostaining in sPRR-His stimulated HK-2 cells (Fig. 6C).

We further assessed the involvement of β-catenin signaling in sPRR-His induced fibrotic response and examined the expression of β-catenin target proteins in HK-2 cells. The FN and β-catenin potential targeted transcription regulator Snail was dramatically increased by sPRR-His treatment in HK-2 cells, upon treating with 10μM β-catenin inhibitor ICG-001, sPRR-His-mediated up-regulation of FN and Snail protein and mRNA abundance were significantly suppressed (Fig. 7A&B). By immunofluorescence, ICG-001 attenuated the deposition of FN induced by sPRR-His (Fig. 7C).

Discussion

The fibrosis has emerged as a critical event in the pathogenesis of ESRD. Knowledge concerning the regulatory mechanism of fibrosis may lead to the development of effective therapies to halt the progression of ESRD**.** The role of PRR in renal fibrosis, as a positive

regulator, has already been reported (20, 29). The present study contributes to the identification the pathological function of sPRR in renal fibrosis.

HK-2 cells are one of the best-characterized renal epithelial cells and have been used by many studies to investigate fibrotic response (39, 45). Under the exposure of TGF-β, a conversion of the epithelial cells to myofibroblasts was induced in HK-2 cells, as evidenced by a complete conversion to spindle-like morphology, the activation of FN, and at same time, this phenomenon was accompanied by the increased generation of sPRR. Inhibiting site-1 protease with PF429242 exhibited a remarkable inhibitory effect on TGF-β induced fibrotic response and sPRR generation. This inhibition was evidenced by an abolishment of FN stimulation, suggesting the potential involvement of sPRR in TGF-β induced fibrotic response. Furthermore, the administration of PF429242 suppressed the TGF-β-induced cell morphological changes in HK-2 cells. Taken together, these findings suggest that sPRR may be a potent positive regulator of TGF-β induced EMT and fibrotic response in HK-2 cells.

What would be the signaling mechanism responsible for sPRR-elicited regulatory effects on fibrotic response? AKT signaling has been associated to the progression and development of TGF-β-induced fibrosis(40). A large amount of studies have proved that AKT signaling mediates fibrosis in different tissues and diseases (11, 12, 14). Therefore, we speculated that sPRR promotes the TGF-β-induced fibrotic response via the stimulation of AKT. As expected, PF429242 remarkably reduced the phosphorylation of AKT, indicating the potential role of AKT signaling in the sPRR contributed fibrotic response.

As a major signaling mediator of fibrosis (20, 25) the potential role of β-catenin was determined. Indeed, PF429242 completely blocked TGF-β induced the nuclear translocation of β-catenin and restored the cytosolic β-catenin. Numerous studies have demonstrated that the

stability of Snail is regulated by Akt(38) and β-catenin(44), and the Snail-mediated FN upregulation is a hallmark of the EMT. After examining the Snail expression, we found that PF429242 remarkably decreased the TGF-β induced Snail stability by suppressing AKT/β-catenin signaling. Overall, these findings favor the notion that sPRR may act via activating AKT/β-catenin/Snail signaling.

To exclude other potential effects of S1P inhibition on fibrotic response, sPRR-His rescue experiment was conducted. As expected, sPRR-His administration reversed the inhibitory effect of PF429242 on FN expression. Meanwhile, after the sPRR-His treatment, we examined the AKT phosphorylation level, β-catenin nuclear translocation and Snail expression in HK-2 cells. Consistent with this observation, sPRR-His restored the inhibitory effect of PF429242 on the phosphorylation level of AKT, promoted the nuclear translocation of β-catenin and elevated the Snail expression of HK-2 cells. However, as evidenced by the unchanged cell morphology, sPRR-His alone was insufficient to induce EMT. The reversed morphological conversion of HK-2 cells by PF429242 treatment indicated that other factors downstream of S1P in addition to sPRR may be needed to induce the full spectrum of EMT. While identity of such factors remains elusive, the sterol regulatory element-binding proteins (SREBPs), which are additional substrates of S1P, may be involved. SREBPs are the transcription factors for lipogenesis genes that could activate genes encoding enzymes of cholesterol and fatty acid biosynthesis(3). Upon the release of SREBPs from the endoplasmic reticulum, a proteolytic activation by S1P in the Golgi was required(3), and the activated SREBPs were reported to be involved in the renal cell injury(16) and EMT transition(42). It seems possible that multiple S1P products such as sPRR and SREBPs may act in concert to induce a full EMT response. This possibility needs to be tested by a separate study in the future.

To explore the TGF-β independent effect of sPRR on fibrotic response, HK-2 cells were

directly treated with sPRR-His. The most striking observation was that sPRR-His in the nanomolar range remarkably induced FN, α-SMA and collagen I expression. However, under the sPRR-His treatment, no changes of E-cadherin protein expression and cell morphology were monitored in HK-2 cells, meaning that sPRR-His could stimulate the fibrotic response, but may not be sufficient to induce EMT. sPRR may act via activation of RAS or direct signaling pathways. In the present study, we tested the role of AT1R in sPRR-His induced fibrotic response in HK-2 cells. Losartan suppressed the FN expression associated with blunted endocytosis of sPRR-His. Thus, the result indicated that sPRR-His-induced fibrotic response is dependent on AT1 receptor-mediated endocytosis. In agreement with this observation, preliminary evidence from Helmy Siragy's group suggests that AT1R and PRR can form a heterodimer that is functionally active to enhance ERK phosphorylation in PC12W cells(32). To explore the underlying mechanism, we examined the involvement of AKT/β-catenin/ Snail signaling pathway. Upon given the PI3K inhibitor LY294002 and β-catenin inhibitor ICG-001 respectively, the sPRR-His induced FN was completely suppressed, companied with the suppression of sPRR-His stimulated Snail expression. It is evident that AKT, β-catenin and Snail are required for the induction of fibrotic response by sPRR-His. Taken together, these observations consolidate the conclusion that AT1R/AKT/β-catenin/Snail signaling pathway is responsible for the sPRR-His induced fibrotic response in HK-2 cells.

In summary, the present study reports an essential role of sPRR in fibrotic response through activating of AKT/β-catenin/Snail pathway. However, sPRR alone is insufficient to induce a full EMT. These findings clarified the role of sPRR in promoting fibrotic response and suggested a new potential therapeutic target of chronic renal disease.

Sources of Funding

This work was supported by the National Natural Science Foundation of China Grants No.

304 81630013 and 81930006. T. Yang is Senior Research Career Scientist in the Department of
305 Veterans Affairs.

306 **Conflict of interest statement**

307 The authors have declared that no conflict of interest exists.

308 **Author Contribution**

309 T Yang and S Xie designed the research; S Xie, J Su, S Mo, Y Lai, M Pu and A Lu performed
310 the experiments; S Xie analyzed the data; S Xie and T Yang wrote the manuscript; all authors
311 approved the final version of the manuscript.

312

Reference

1. **Bakin AV, Tomlinson AK, Bhowmick NA, Moses HL, and Arteaga CL**. Phosphatidylinositol 3-kinase function is required for transforming growth factor beta-mediated epithelial to mesenchymal transition and cell migration. *J Biol Chem* 275: 36803-36810, 2000.

2. **Border WA, Okuda S, Languino LR, Sporn MB, and Ruoslahti E**. Suppression of experimental glomerulonephritis by antiserum against transforming growth factor beta 1. *Nature* 346: 371-374, 1990.

3. **Brown MS, and Goldstein JL**. A proteolytic pathway that controls the cholesterol content of membranes, cells, and blood. *Proc Natl Acad Sci U S A* 96: 11041-11048, 1999.

4. **Burckle C, and Bader M**. Prorenin and its ancient receptor. *Hypertension* 48: 549-551, 2006.

5. **Castaneda A, Serrano C, Hernandez-Trejo JA, Gutierrez-Martinez IZ, Montejo-Lopez W, Gomez-Suarez M, Hernandez-Ruiz M, Betanzos A, Candelario-Martinez A, Romo-Parra H, Arias-Montano JA, Schnoor M, Meraz Rios MA, Gutierrez-Castillo ME, Martinez-Davila IA, Villegas-Sepulveda N, Martinez-Fong D, and Nava P**. pVHL suppresses Akt/beta-catenin-mediated cell proliferation by inhibiting 14-3-3zeta expression. *Biochem J* 474: 2679-2689, 2017.

6. **Connelly KA, Advani A, Kim S, Advani SL, Zhang M, White KE, Kim YM, Parker C, Thai K, Krum H, Kelly DJ, and Gilbert RE**. The cardiac (pro)renin receptor is primarily expressed in myocyte transverse tubules and is increased in experimental diabetic cardiomyopathy. *J Hypertens* 29: 1175-1184, 2011.

7. **Cousin C, Bracquart D, Contrepas A, Corvol P, Muller L, and Nguyen G**. Soluble form of the (pro)renin receptor generated by intracellular cleavage by furin is secreted in plasma. *Hypertension* 53: 1077-1082, 2009.

8. **Gatineau E, Cohn DM, Poglitsch M, Loria AS, Gong M, and Yiannikouris F**. Losartan prevents the elevation of blood pressure in adipose-PRR deficient female mice while elevated circulating sPRR activates the renin-angiotensin system. *Am J Physiol Heart Circ Physiol* 316: H506-H515, 2019.

9. **Gatineau E, Gong MC, and Yiannikouris F**. Soluble Prorenin Receptor Increases Blood Pressure in High Fat-Fed Male Mice. *Hypertension* 74: 1014-1020, 2019.

10. **Hamidi A, Song J, Thakur N, Itoh S, Marcusson A, Bergh A, Heldin CH, and Landstrom M**. TGF-beta promotes PI3K-AKT signaling and prostate cancer cell migration through the TRAF6-mediated ubiquitylation of p85alpha. *Sci Signal* 10: 2017.

11. **Higgins DF, Ewart LM, Masterson E, Tennant S, Grebnev G, Prunotto M, Pomposiello S, Conde-Knape K, Martin FM, and Godson C**. BMP7-induced-Pten inhibits Akt and prevents renal fibrosis. *Biochim Biophys Acta Mol Basis Dis* 1863: 3095-3104, 2017.

12. **Hongtao C, Youling F, Fang H, Huihua P, Jiying Z, and Jun Z**. Curcumin alleviates

ischemia reperfusion-induced late kidney fibrosis through the APPL1/Akt signaling pathway. *J Cell Physiol* 233: 8588-8596, 2018.

13. **Humphreys BD**. Mechanisms of Renal Fibrosis. *Annu Rev Physiol* 80: 309-326, 2018.

14. **Imamura M, Moon JS, Chung KP, Nakahira K, Muthukumar T, Shingarev R, Ryter SW, Choi AM, and Choi ME**. RIPK3 promotes kidney fibrosis via AKT-dependent ATP citrate lyase. *JCI Insight* 3: 2018.

15. **Isaka Y**. Targeting TGF-beta Signaling in Kidney Fibrosis. *Int J Mol Sci* 19: 2018.

16. **Lhotak S, Sood S, Brimble E, Carlisle RE, Colgan SM, Mazzetti A, Dickhout JG, Ingram AJ, and Austin RC**. ER stress contributes to renal proximal tubule injury by increasing SREBP-2-mediated lipid accumulation and apoptotic cell death. *Am J Physiol Renal Physiol* 303: F266-278, 2012.

17. **Li W, Peng H, Cao T, Sato R, McDaniels SJ, Kobori H, Navar LG, and Feng Y**. Brain-targeted (pro)renin receptor knockdown attenuates angiotensin II-dependent hypertension. *Hypertension* 59: 1188-1194, 2012.

18. **Li W, Sullivan MN, Zhang S, Worker CJ, Xiong Z, Speth RC, and Feng Y**. Intracerebroventricular infusion of the (Pro)renin receptor antagonist PRO20 attenuates deoxycorticosterone acetate-salt-induced hypertension. *Hypertension* 65: 352-361, 2015.

19. **Li Y, Tan X, Dai C, Stolz DB, Wang D, and Liu Y**. Inhibition of integrin-linked kinase attenuates renal interstitial fibrosis. *J Am Soc Nephrol* 20: 1907-1918, 2009.

20. **Li Z, Zhou L, Wang Y, Miao J, Hong X, Hou FF, and Liu Y**. (Pro)renin Receptor Is an Amplifier of Wnt/beta-Catenin Signaling in Kidney Injury and Fibrosis. *J Am Soc Nephrol* 28: 2393-2408, 2017.

21. **Liu Y**. Cellular and molecular mechanisms of renal fibrosis. *Nat Rev Nephrol* 7: 684-696, 2011.

22. **Lopez-Rodriguez E, Boden C, Echaide M, Perez-Gil J, Kolb M, Gauldie J, Maus UA, Ochs M, and Knudsen L**. Surfactant dysfunction during overexpression of TGF-beta1 precedes profibrotic lung remodeling in vivo. *Am J Physiol Lung Cell Mol Physiol* 310: L1260-1271, 2016.

23. **Lu X, Wang F, Xu C, Soodvilai S, Peng K, Su J, Zhao L, Yang KT, Feng Y, Zhou SF, Gustafsson JA, and Yang T**. Soluble (pro)renin receptor via beta-catenin enhances urine concentration capability as a target of liver X receptor. *Proc Natl Acad Sci U S A* 113: E1898-1906, 2016.

24. **Mahmud H, Sillje HH, Cannon MV, van Gilst WH, and de Boer RA**. Regulation of the (pro)renin-renin receptor in cardiac remodelling. *J Cell Mol Med* 16: 722-729, 2012.

25. **Mencke R, Olauson H, and Hillebrands JL**. Effects of Klotho on fibrosis and cancer: A renal focus on mechanisms and therapeutic strategies. *Adv Drug Deliv Rev* 121: 85-100, 2017.

26. **Moon JA, Kim HT, Cho IS, Sheen YY, and Kim DK**. IN-1130, a novel transforming

388 growth factor-beta type I receptor kinase (ALK5) inhibitor, suppresses renal fibrosis in
389 obstructive nephropathy. *Kidney Int* 70: 1234-1243, 2006.

390 27. **Nakagawa T, Suzuki-Nakagawa C, Watanabe A, Asami E, Matsumoto M, Nakano**
391 **M, Ebihara A, Uddin MN, and Suzuki F**. Site-1 protease is required for the generation of
392 soluble (pro)renin receptor. *J Biochem* 161: 369-379, 2017.

393 28. **Narita T, Ichihara A, Matsuoka K, Takai Y, Bokuda K, Morimoto S, Itoh H, and**
394 **Seki H**. Placental (pro)renin receptor expression and plasma soluble (pro)renin receptor levels
395 in preeclampsia. *Placenta* 37: 72-78, 2016.

396 29. **Narumi K, Sato E, Hirose T, Yamamoto T, Nakamichi T, Miyazaki M, Sato H, and**
397 **Ito S**. (Pro)renin receptor is involved in mesangial fibrosis and matrix expansion. *Sci Rep* 8:
398 16, 2018.

399 30. **Nguyen G, Delarue F, Burckle C, Bouzhir L, Giller T, and Sraer JD**. Pivotal role of
400 the renin/prorenin receptor in angiotensin II production and cellular responses to renin. *J Clin*
401 *Invest* 109: 1417-1427, 2002.

402 31. **Peng K, Lu X, Wang F, Nau A, Chen R, Zhou SF, and Yang T**. Collecting duct
403 (pro)renin receptor targets ENaC to mediate angiotensin II-induced hypertension. *Am J*
404 *Physiol Renal Physiol* 312: F245-F253, 2017.

405 32. **Quadri SSA, Li C, Culver S, and Siragy HM**. Abstract P099: Angiotensin Type I
406 Receptor (AT1R) and (Pro)renin Receptor (PRR) Functional Heterodimer Mediates ERK
407 Phosphorylation. *Hypertension* 66: AP099, 2015.

408 33. **Riquier-Brison ADM, Sipos A, Prokai A, Vargas SL, Toma L, Meer EJ, Villanueva**
409 **KG, Chen JCM, Gyarmati G, Yih C, Tang E, Nadim B, Pendekanti S, Garrelds IM,**
410 **Nguyen G, Danser AHJ, and Peti-Peterdi J**. The macula densa prorenin receptor is
411 essential in renin release and blood pressure control. *Am J Physiol Renal Physiol* 315:
412 F521-F534, 2018.

413 34. **Rosenbloom J, Castro SV, and Jimenez SA**. Narrative review: fibrotic diseases:
414 cellular and molecular mechanisms and novel therapies. *Ann Intern Med* 152: 159-166, 2010.

415 35. **Russo LM, del Re E, Brown D, and Lin HY**. Evidence for a role of transforming
416 growth factor (TGF)-beta1 in the induction of postglomerular albuminuria in diabetic
417 nephropathy: amelioration by soluble TGF-beta type II receptor. *Diabetes* 56: 380-388, 2007.

418 36. **Sureshbabu A, Muhsin SA, and Choi ME**. TGF-beta signaling in the kidney:
419 profibrotic and protective effects. *Am J Physiol Renal Physiol* 310: F596-F606, 2016.

420 37. **Vega G, Alarcon S, and San Martin R**. The cellular and signalling alterations
421 conducted by TGF-beta contributing to renal fibrosis. *Cytokine* 88: 115-125, 2016.

422 38. **Wang H, Zhang G, Zhang H, Zhang F, Zhou B, Ning F, Wang HS, Cai SH, and Du**
423 **J**. Acquisition of epithelial-mesenchymal transition phenotype and cancer stem cell-like
424 properties in cisplatin-resistant lung cancer cells through AKT/beta-catenin/Snail signaling
425 pathway. *Eur J Pharmacol* 723: 156-166, 2014.

426 39. **Wang J, Pan J, Li H, Long J, Fang F, Chen J, Zhu X, Xiang X, and Zhang D**.
427 lncRNA ZEB1-AS1 Was Suppressed by p53 for Renal Fibrosis in Diabetic Nephropathy. *Mol*
428 *Ther Nucleic Acids* 12: 741-750, 2018.

429 40. **Wang JL, Chen CW, Tsai MR, Liu SF, Hung TJ, Yu Ju H, Chang WT, Shi MD,**
430 **Hsieh PF, and Yang YL**. Antifibrotic role of PGC-1alpha-siRNA against
431 TGF-beta1-induced renal interstitial fibrosis. *Exp Cell Res* 370: 160-167, 2018.

432 41. **Wang X, Chen H, Tian R, Zhang Y, Drutskaya MS, Wang C, Ge J, Fan Z, Kong D,**
433 **Wang X, Cai T, Zhou Y, Wang J, Wang J, Wang S, Qin Z, Jia H, Wu Y, Liu J,**
434 **Nedospasov SA, Tredget EE, Lin M, Liu J, Jiang Y, and Wu Y**. Macrophages induce
435 AKT/beta-catenin-dependent Lgr5(+) stem cell activation and hair follicle regeneration
436 through TNF. *Nat Commun* 8: 14091, 2017.

437 42. **Wang Y, Wang H, Zhao Q, Xia Y, Hu X, and Guo J**. PD-L1 induces
438 epithelial-to-mesenchymal transition via activating SREBP-1c in renal cell carcinoma. *Med*
439 *Oncol* 32: 212, 2015.

440 43. **Zhang YE**. Non-Smad pathways in TGF-beta signaling. *Cell Res* 19: 128-139, 2009.

441 44. **Zhao J, Ou B, Han D, Wang P, Zong Y, Zhu C, Liu D, Zheng M, Sun J, Feng H, and**
442 **Lu A**. Tumor-derived CXCL5 promotes human colorectal cancer metastasis through
443 activation of the ERK/Elk-1/Snail and AKT/GSK3beta/beta-catenin pathways. *Mol Cancer* 16:
444 70, 2017.

445 45. **Zhou B, Mu J, Gong Y, Lu C, Zhao Y, He T, and Qin Z**. Brd4 inhibition attenuates
446 unilateral ureteral obstruction-induced fibrosis by blocking TGF-beta-mediated Nox4
447 expression. *Redox Biol* 11: 390-402, 2017.

448

Figure Legends

Fig. 1. TGF-β induced fibrosis and sPRR generation in HK2 cells. The cells were grown on 6-well plates until 80% confluence and then treated with 10ng/ml TGF-β for 24h. fPRR, sPRR and FN protein expression was analyzed by immunoblotting and analyzed by densitometry analysis (A). ELISA measurement of medium sPRR and normalized by protein content (B). FN mRNA level was determined by RT-qPCR (C). Morphologic changes of HK-2 cells, photographs were taken using a Nikon microscope (D). Immunostaining detection of FN expression and DAPI, Scale bars indicate 50μm (E). Statistical significance was determined by using unpaired Student's *t* test. **P* < 0.05 versus CTR; ***P* < 0.01 versus CTR.

Fig. 2. S1P inhibitor PF429242 suppressed TGF-β induced sPRR generation and fibrosis in HK-2 cells. The cells were grown on 6-well plates until 80% confluence, pretreated with 40 μM PF429242 and the treated with 10ng/ml TGF-β for 24h. fPRR, sPRR and FN protein expression were analyzed by immunoblotting and densitometry analysis (A). ELISA measurement of medium sPRR and normalized by protein content (B). HK-2 cells were pretreated with 40 μM PF429242 alone, and then treated with 10ng/ml TGF-β for 15min. p-AKT and T-AKT protein expression were analyzed by immunoblotting and densitometry analysis (C). Immunoblotting analysis of nuclear and cytosolic β-catenin abundance (D&E). Snail protein expression were analyzed by immunoblotting and densitometry analysis (F). RT-qPCR detection of FN, Snail and S1P mRNA levels (G). Morphologic changes of HK-2 cells, photographs were taken using a Nikon microscope (H). FN expression and DAPI was determined by immunostaining, Scale bars indicate 50μm (I). Statistical significance was determined by using unpaired Student's *t* test. **P* < 0.05 versus CTR; ***P* < 0.01 versus CTR; $^{\#}P < 0.05$ versus TGF-β; $^{\#\#}P < 0.01$ versus TGF-β.

Fig. 3. sPRR-His reversed PF429242 suppressed fibrosis via AKT/β-catenin/Snail pathway in TGF-β stimulated HK2 cells. The cells were grown on 6-well plates until 80% confluence, pretreated with 40 μM PF429242 alone or in combination with 60nM sPRR-His, and then treated with 10ng/ml TGF-β for 24h. fPRR, sPRR and FN protein expression was analyzed by immunoblotting and densitometry analysis (A). ELISA measurement of medium sPRR and normalized protein content (B). HK-2 cells were pretreated with 40 μM PF429242 alone alone or in combination with 60nM sPRR-His, and then treated with 10ng/ml TGF-β for 15min. p-AKT and T-AKT protein expression were analyzed by immunoblotting and densitometry analysis (C). Immunoblotting analysis of nuclear and cytosolic β-catenin abundance (D&E). Snail protein expression was analyzed by immunoblotting and densitometry analysis (F). RT-qPCR detection of FN, Snail and S1P mRNA levels (G). Morphologic changes of HK-2 cells, photographs were taken using a Nikon microscope (H). FN expression and DAPI was detected by immunostaining, Scale bars indicate 50μm (I). Statistical significance was determined by using unpaired Student's *t* test. $^{*}P < 0.05$ versus CTR; $^{**}P < 0.01$ versus CTR; $^{\#}P < 0.05$ versus TGF-β; $^{\#\#}P < 0.01$ versus TGF-β; $^{\&}P < 0.05$ versus TGF-β+PF429242; $^{\&\&}P < 0.01$ versus TGF-β+PF429242.

Fig. 4. sPRR-His directly promotes fibrosis in HK2 cells. The cells were grown on 6-well plates until 80% confluence and then treated with 60 nM sPRR-His for 36h. FN, p-AKT, T-AKT and Snail protein expression was analyzed by immunoblotting and densitometry analysis (A). RT-qPCR determination of FN and Snail mRNA levels (B). Immunoblotting analysis of α-SMA, Collagen I and E-cadherin abundance (C). Morphologic changes of HK-2

cells, photographs were taken using a Nikon microscope (D). Immunofluorescence staining of FN and DAPI, Scale bars indicate 50μm (E). Statistical significance was determined by using unpaired Student's *t* test. **P* < 0.05 versus CTR; ***P* < 0.01 versus CTR.

Fig. 5. AT1 receptor inhibitor Losartan blocked sPRR-His endocytosis and the induced fibrosis in HK-2 cells. The cells were grown on 6-well plates until 80% confluence, pretreated with 10 μM Losartan, and then treated with 60 nM sPRR-His for 36h. fPRR, sPRR-His, FN, p-AKT, T-AKT and Snail protein expression was analyzed by immunoblotting and densitometry analysis (A). RT-qPCR determination of FN and Snail mRNA levels (B). Immunofluorescence staining of FN and DAPI, Scale bars indicate 50μm (C). Statistical significance was determined by using unpaired Student's *t* test. **P* < 0.05 versus CTR; ***P* < 0.01 versus CTR; $^{\#}P$ < 0.05 versus sPRR-His; $^{\#\#}P$ < 0.01 versus sPRR-His.

Fig. 6. PI3K inhibitor LY294002 attenuated sPRR-His induce fibrosis in HK-2 cells. The cells were grown on 6-well plates until 80% confluence, pretreated with 10 μM LY294002, and then treated with 60 nM sPRR-His for 36h. FN, p-AKT, T-AKT and Snail protein expression was analyzed by immunoblotting and densitometry analysis (A). RT-qPCR determination of FN and Snail mRNA levels (B). Immunofluorescence staining of FN and DAPI, Scale bars indicate 50μm (C). Statistical significance was determined by using unpaired Student's *t* test. **P* < 0.05 versus CTR; ***P* < 0.01 versus CTR; $^{\#}P$ < 0.05 versus sPRR-His; $^{\#\#}P$ < 0.01 versus sPRR-His.

Fig. 7. β-catenin inhibitor ICG-001 reduced sPRR-His induce fibrosis in HK-2 cells. The cells were grown on 6-well plates until 80% confluence, pretreated with 10 μM ICG-001, and then treated with 60 nM sPRR-His for 36h. FN, p-AKT, T-AKT and Snail protein expression was analyzed by immunoblotting and densitometry analysis (A). RT-qPCR determination of FN and Snail mRNA levels (B). Immunofluorescence staining of FN and DAPI, Scale bars indicate 50μm (C). Statistical significance was determined by using unpaired Student's *t* test. $*P < 0.05$ versus CTR; $**P < 0.01$ versus CTR; $^{\#}P < 0.05$ versus sPRR-His; $^{\#\#}P < 0.01$ versus sPRR-His.

Figure 1

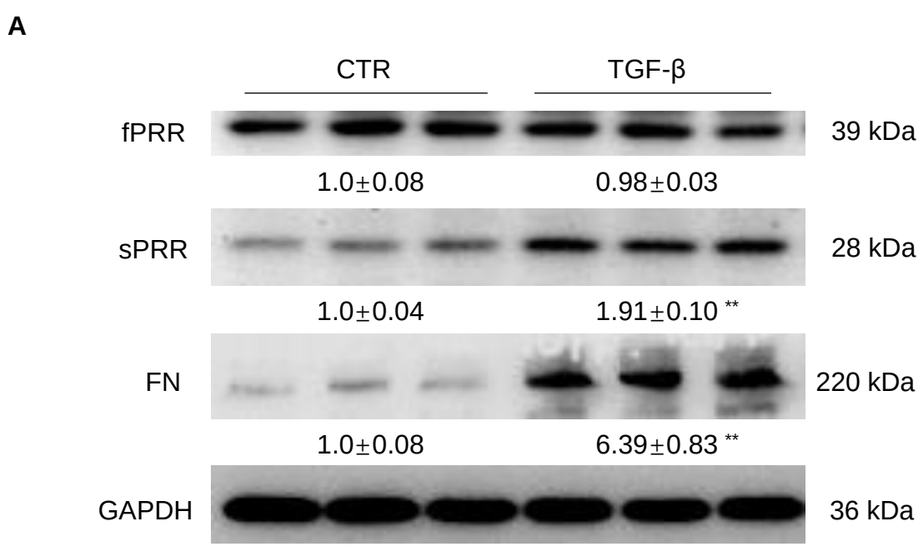

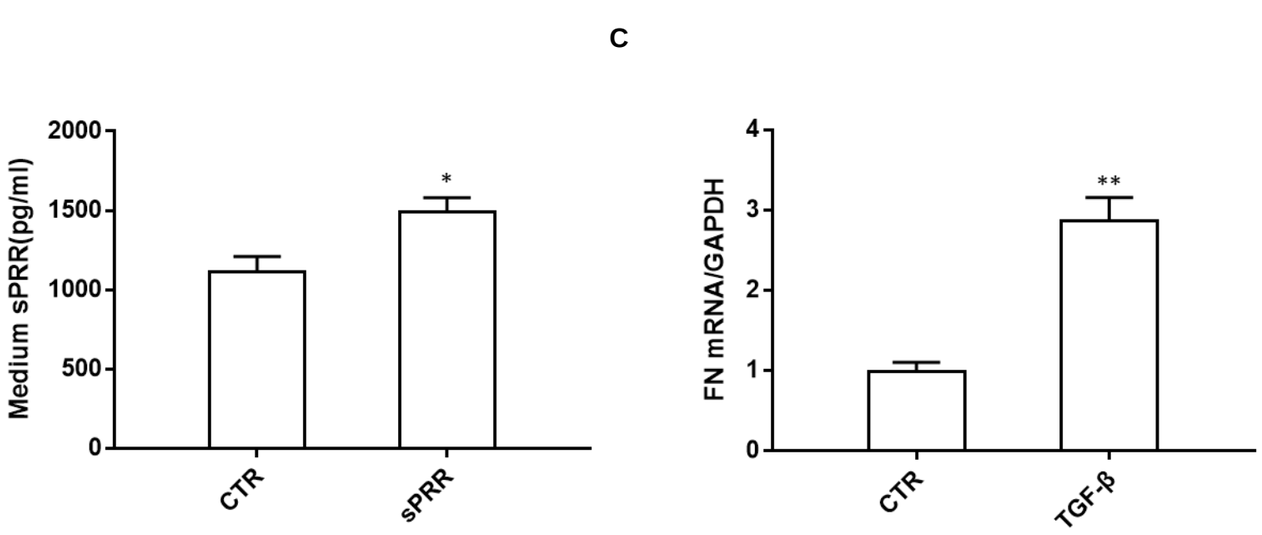

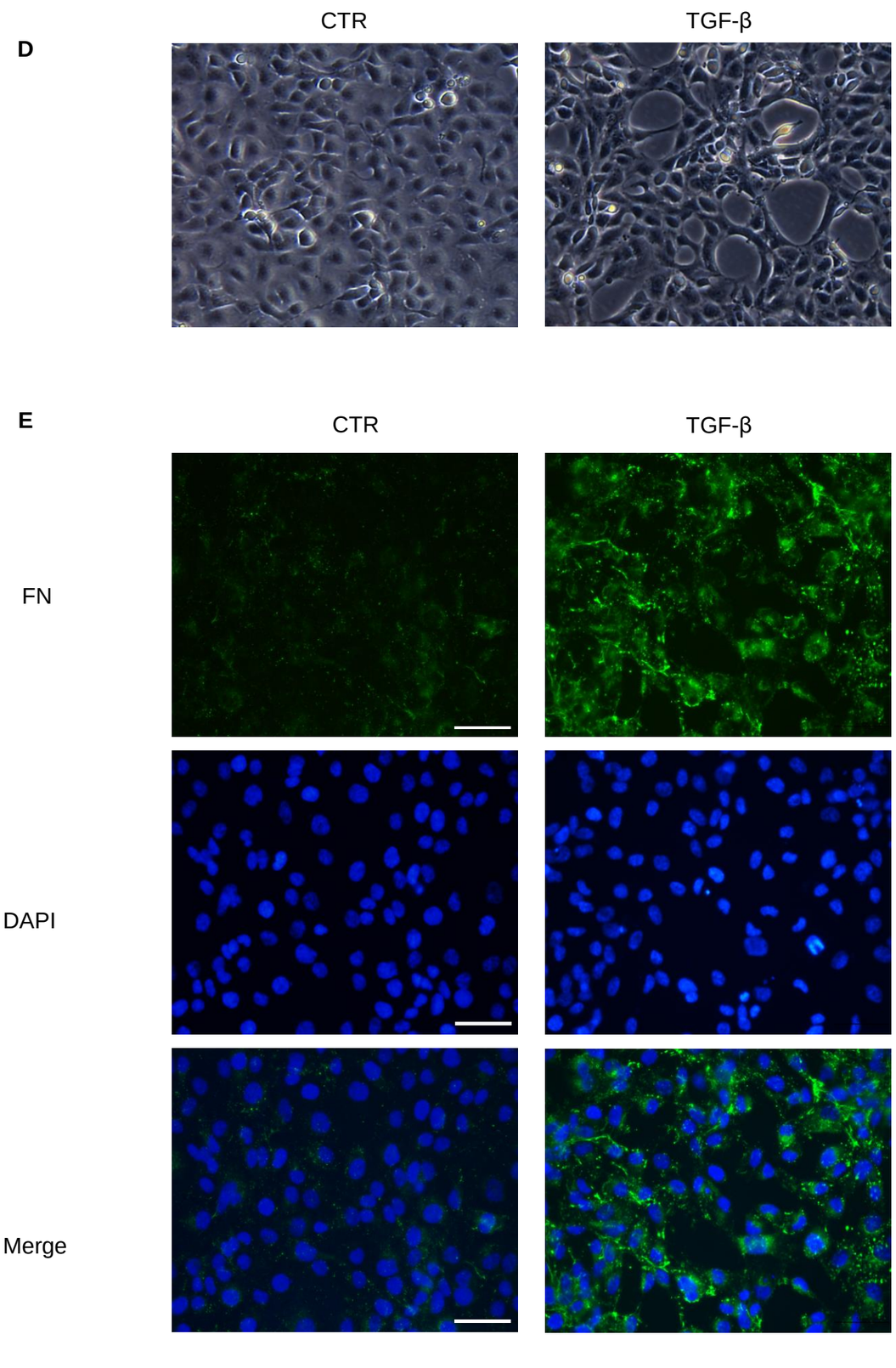

Figure 2

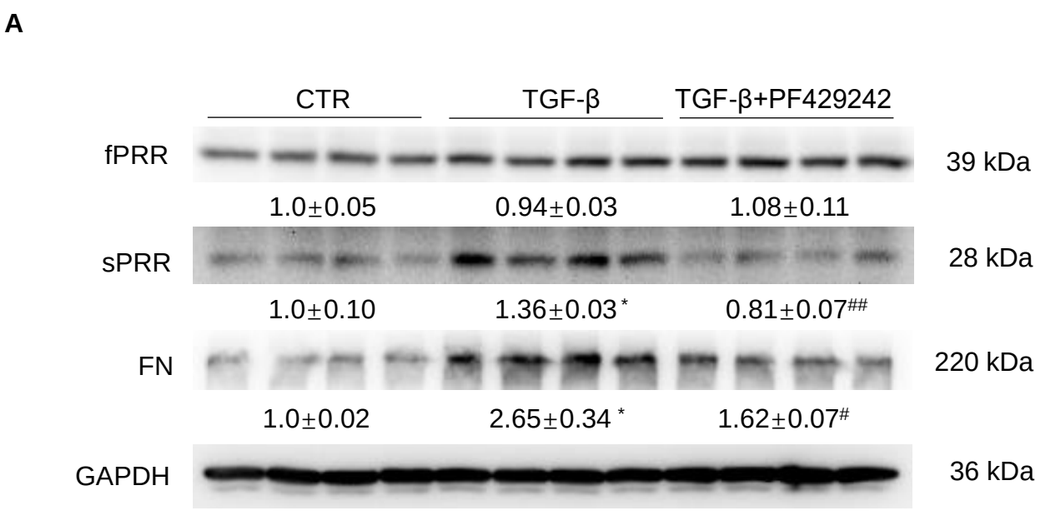

Figure 3

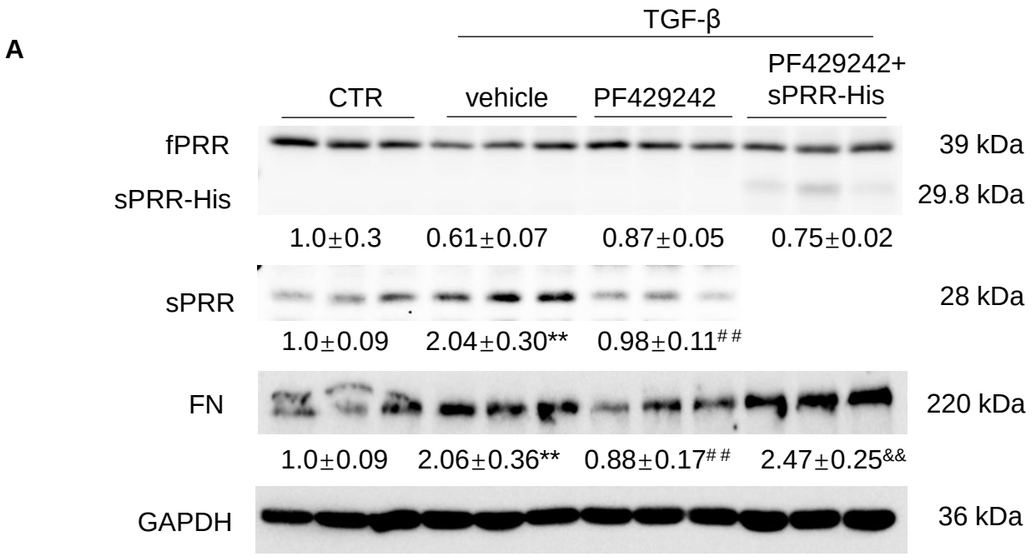

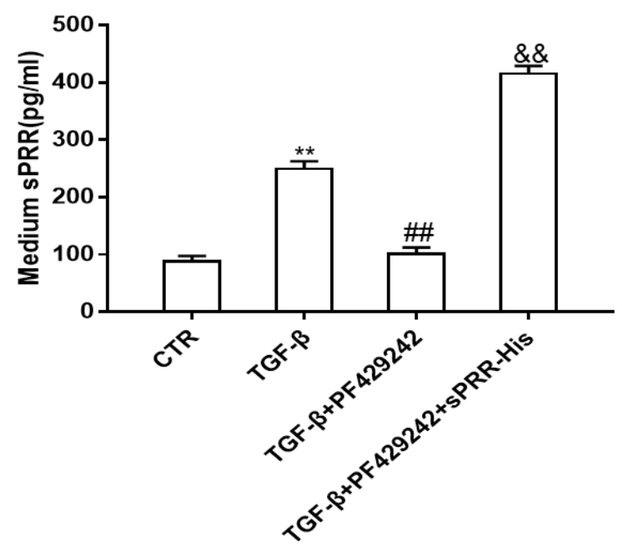

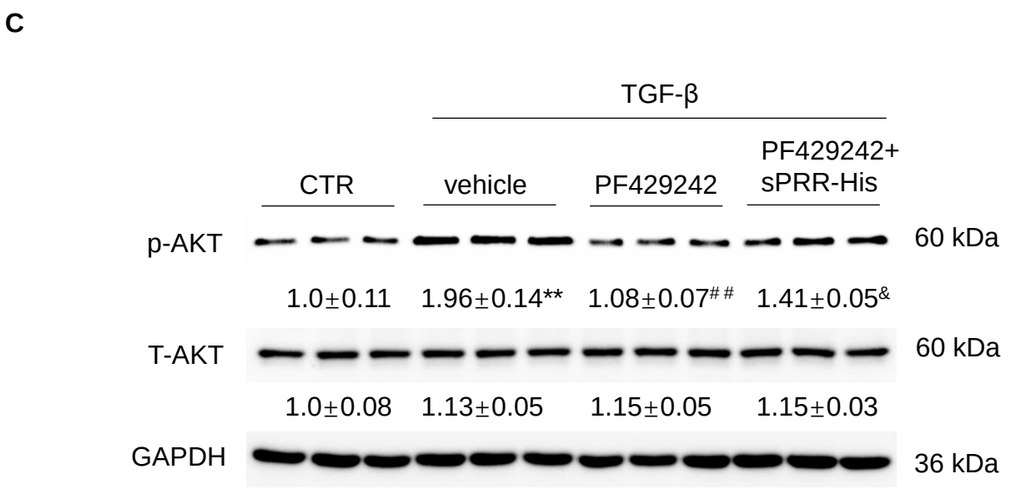

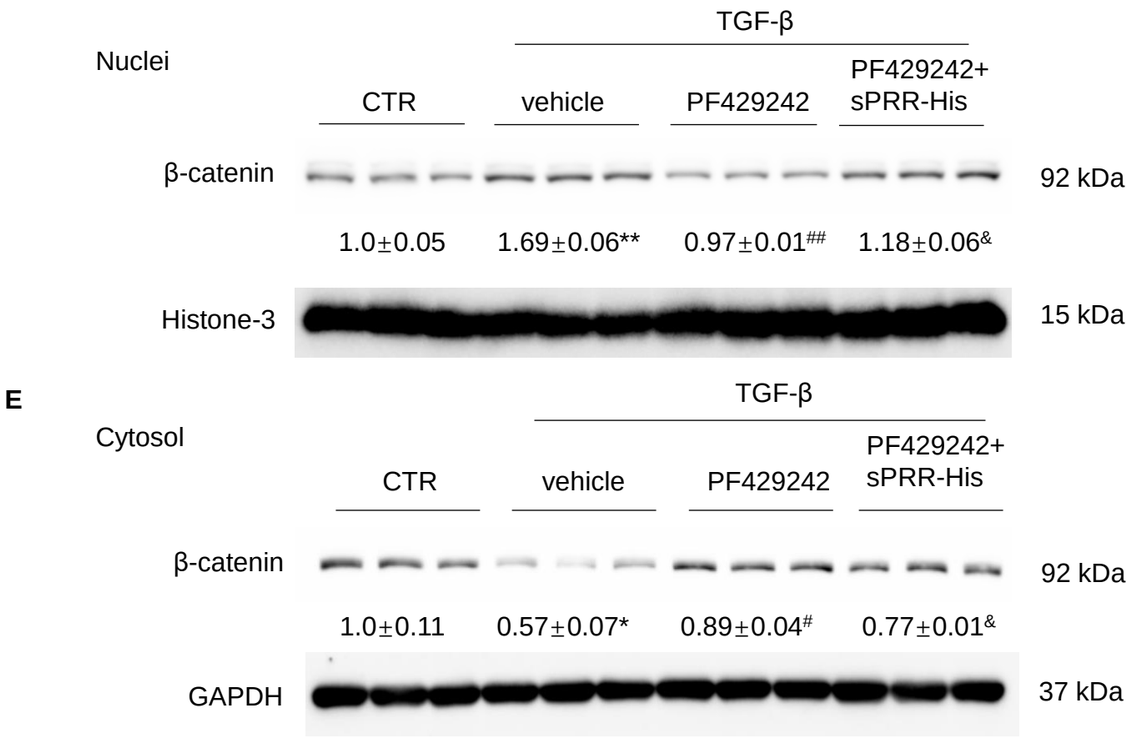

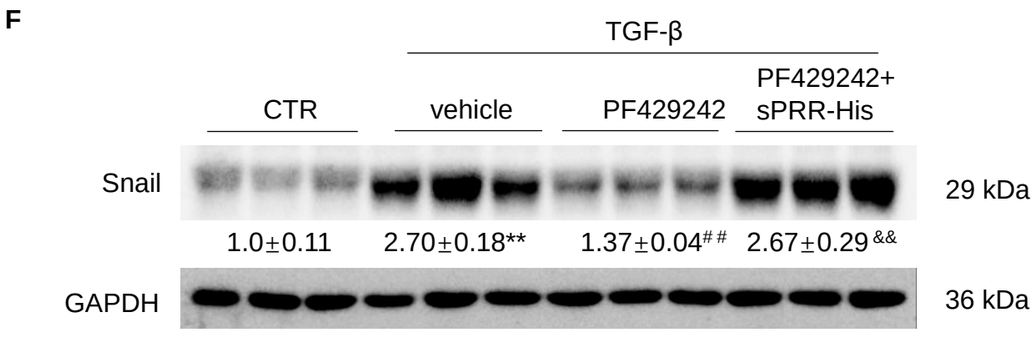

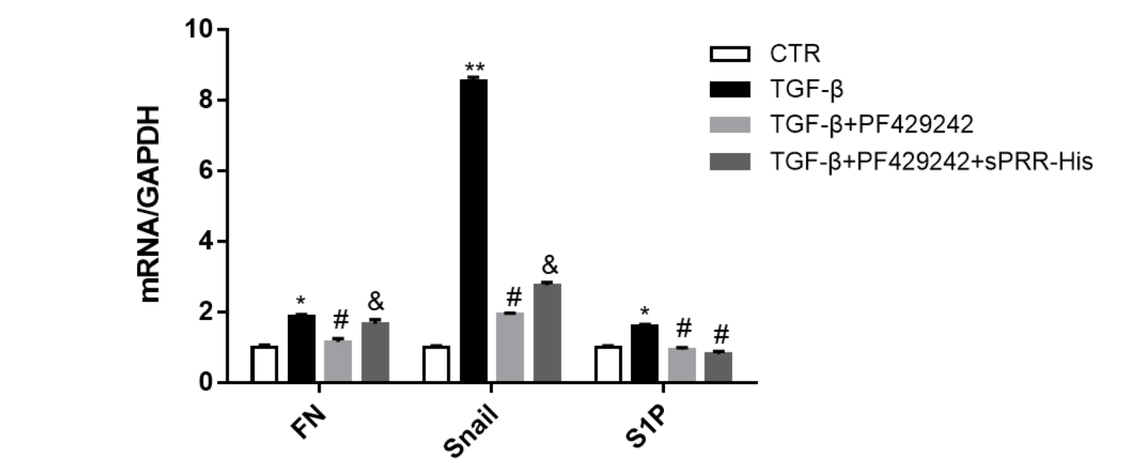

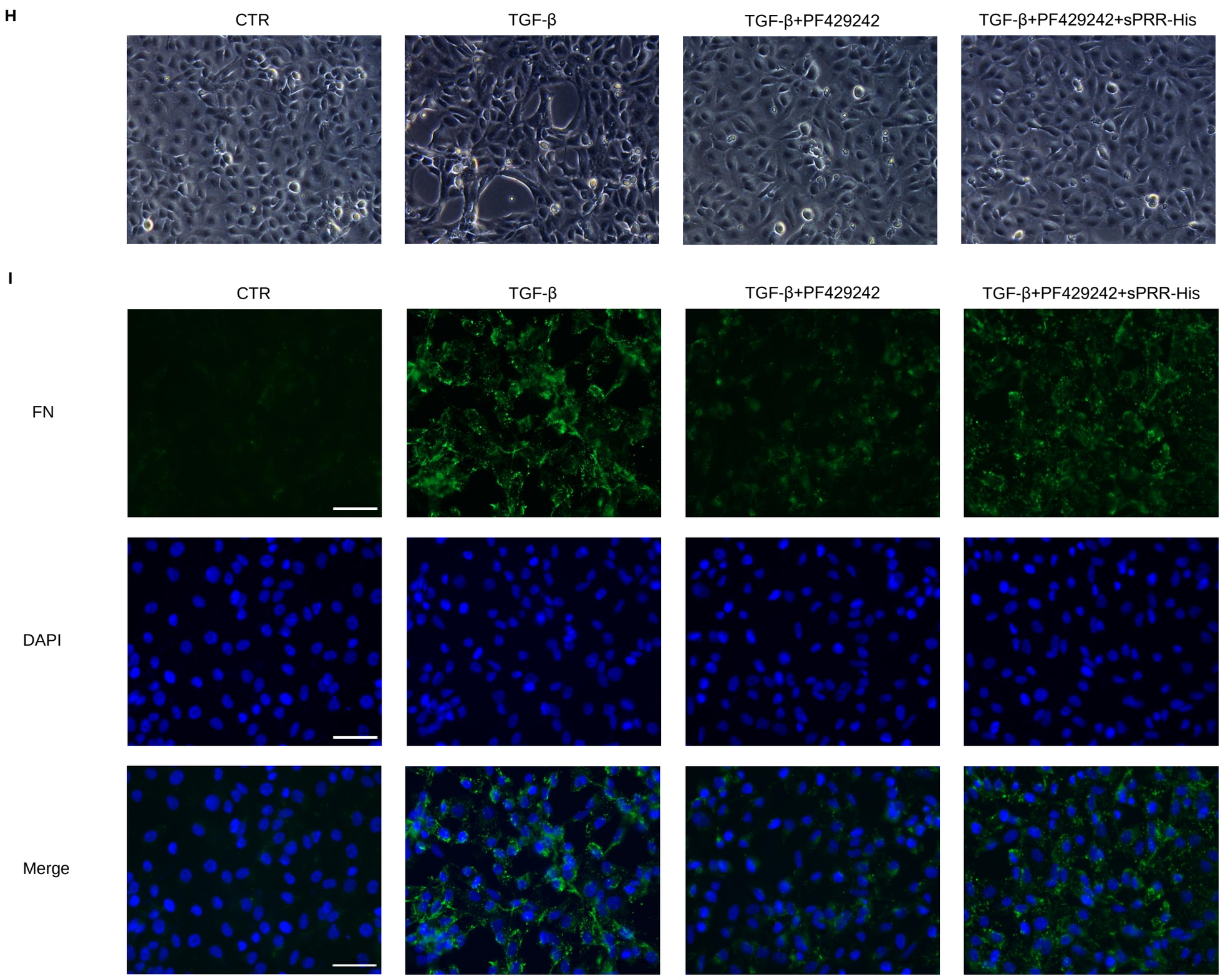

Figure 4

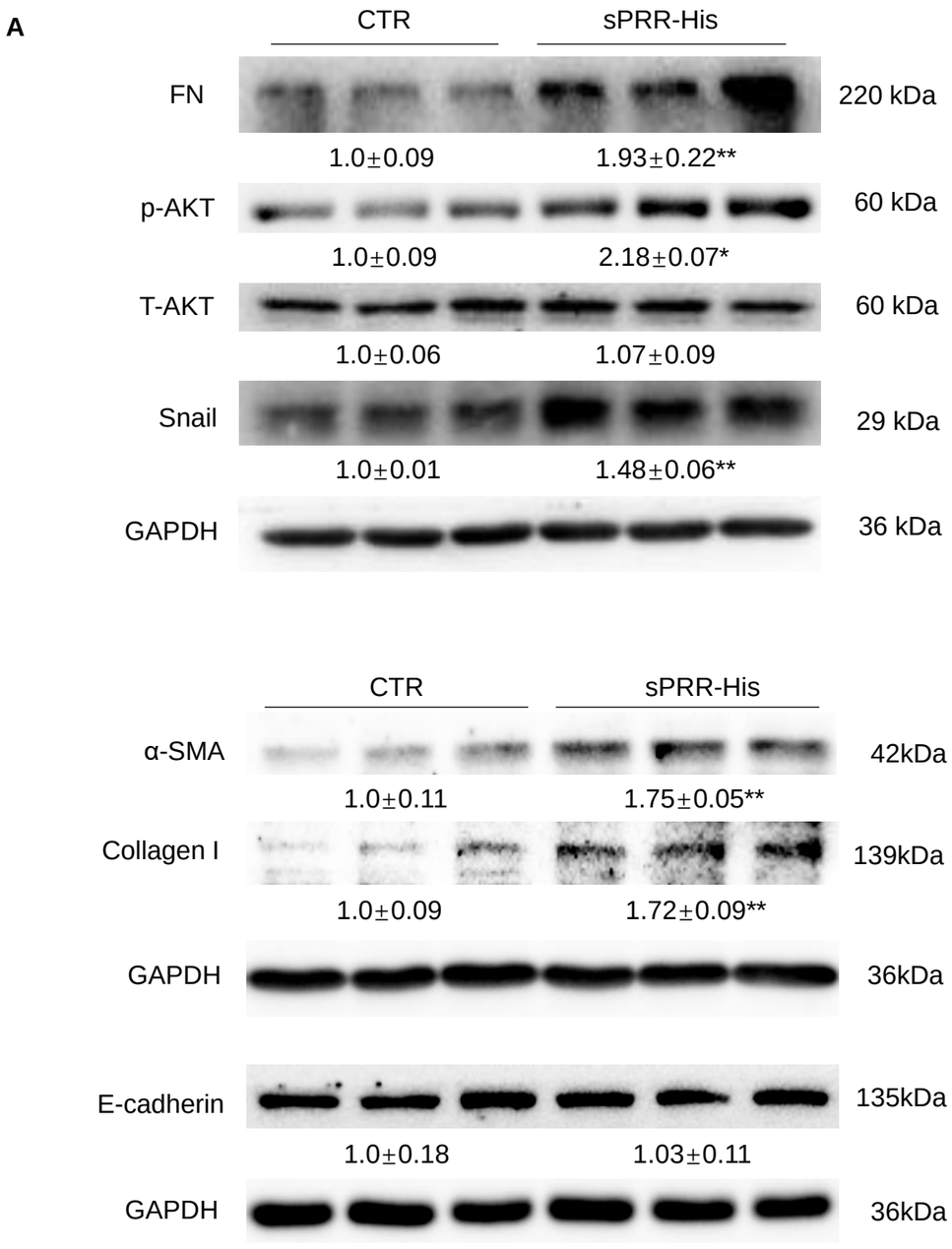

Figure 5

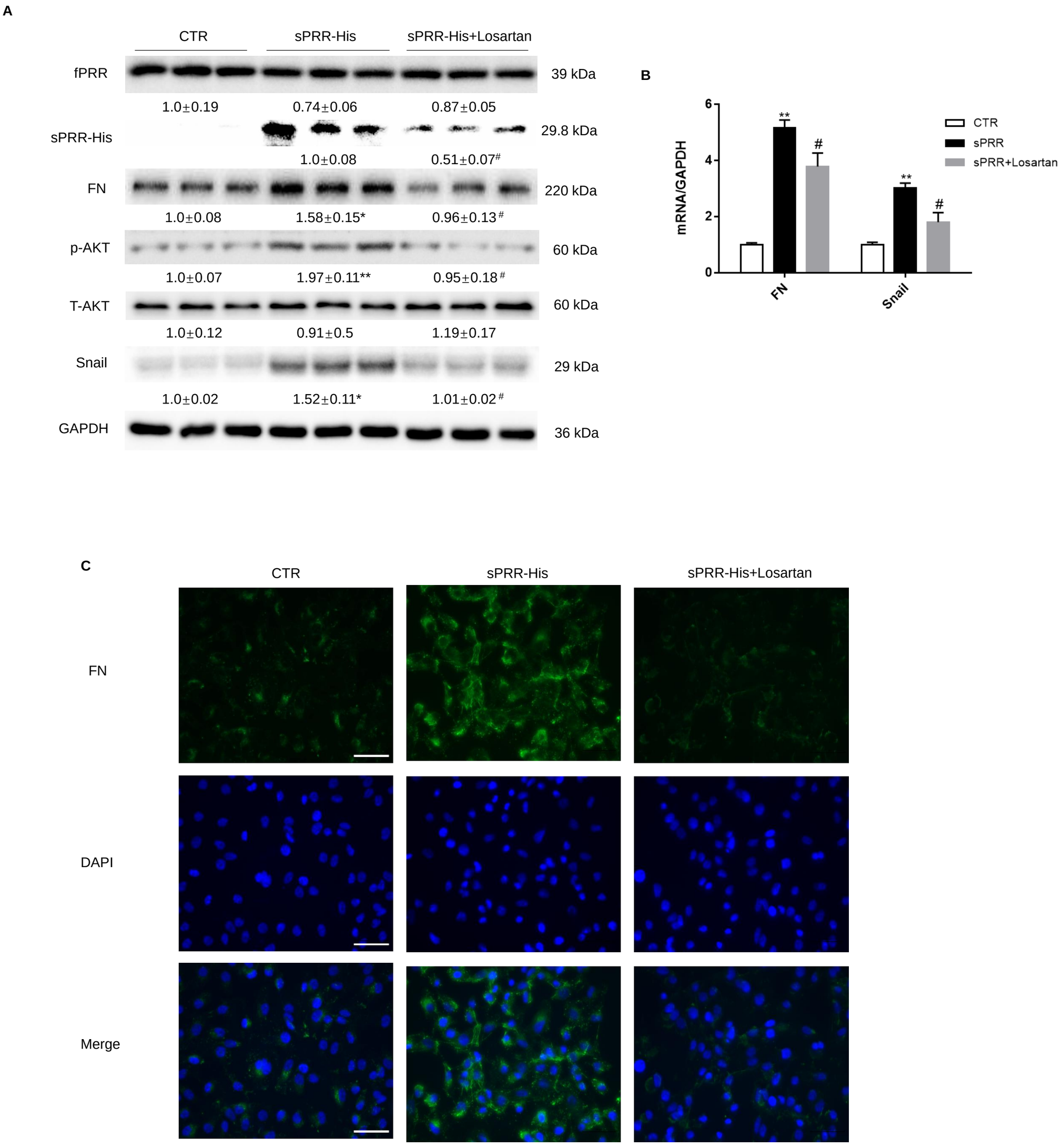

Figure 6

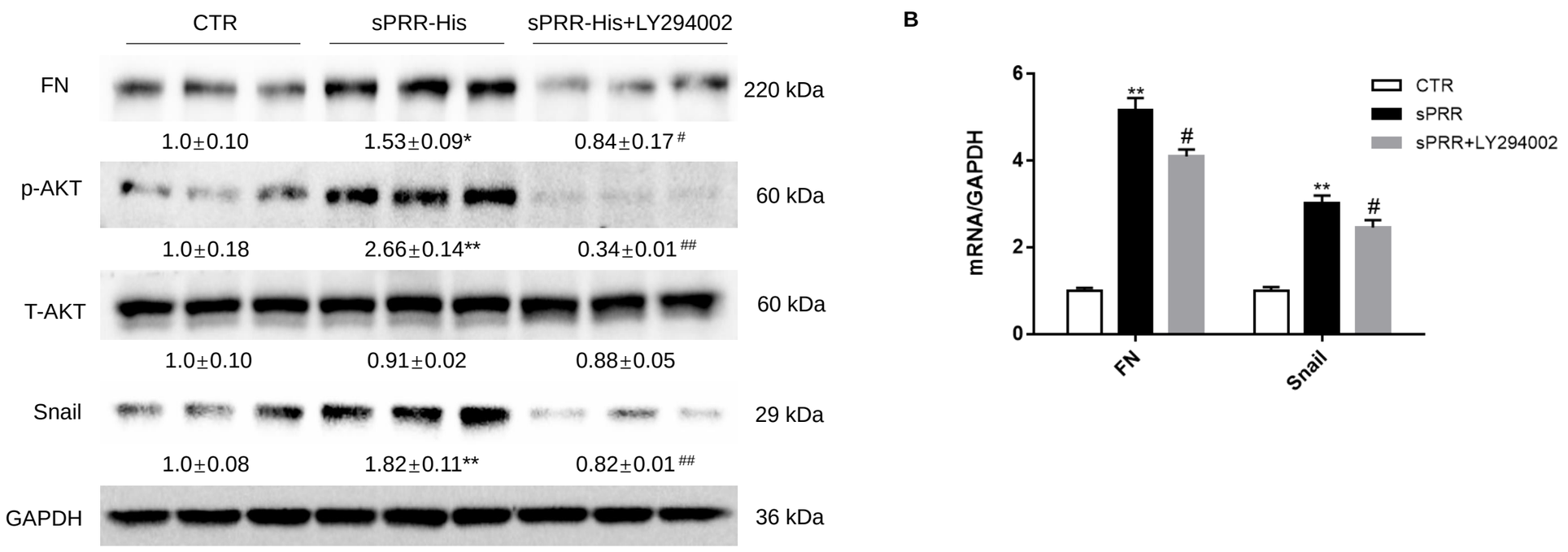

Figure 7

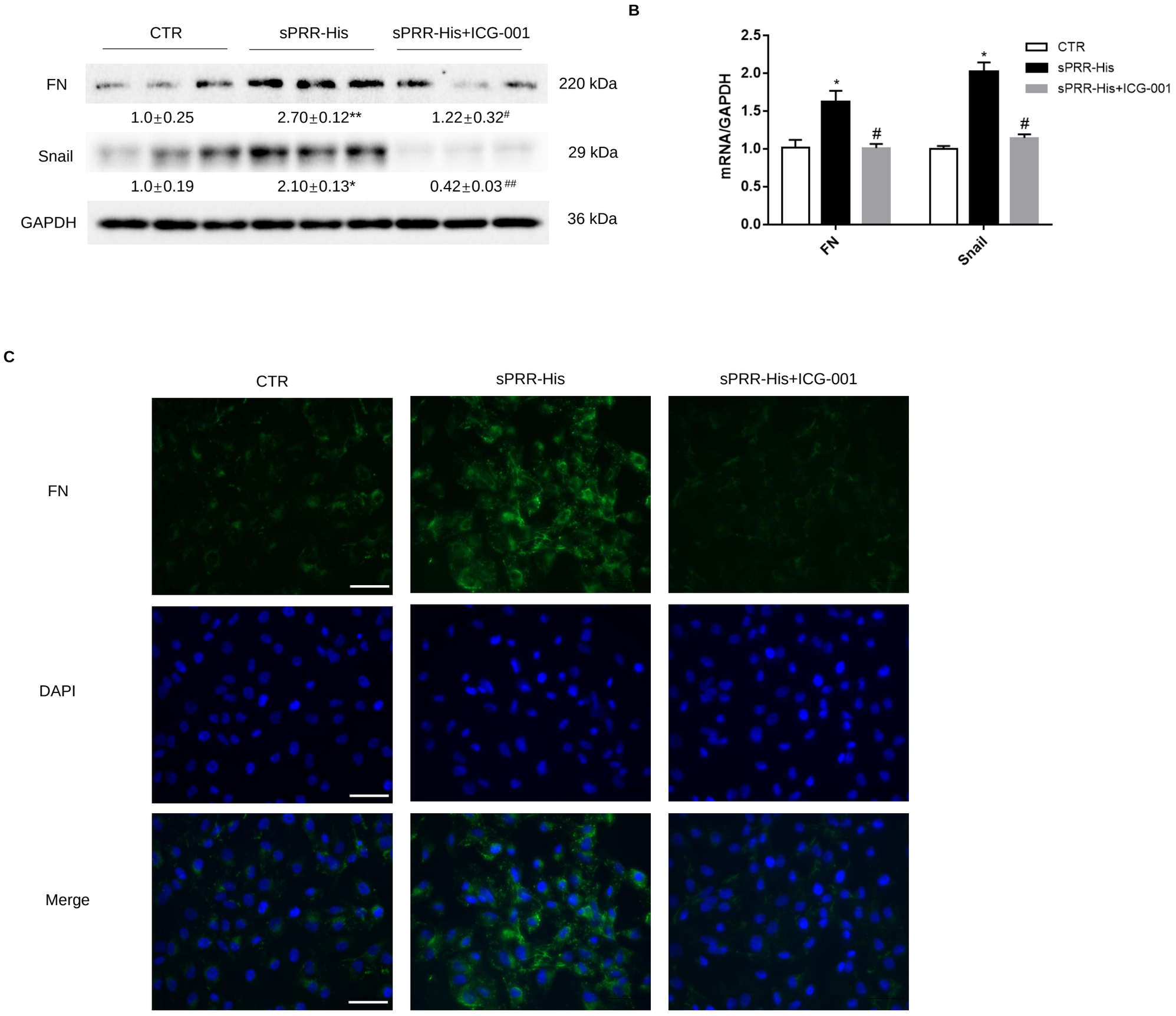

Soluble (pro)renin receptor promotes fibrotic response in renal proximal tubule epithelial cells in vitro via Akt/β-catenin/Snail signaling pathway

METHODS

1. TGF-β was used to induce fibrotic response and sPRR generation in HK-2 cells.
2. To confirm the role of sPRR in TGF-β stimulated fibrotic response, site-1 protease inhibitor PF429242 was used to block sPRR production, and then sPRR-His was administrated to restore the sPRR concentration.
3. sPRR-His could stimulate fibrotic response directly, losartan, LY294002 and ICG were used to detect the involvement of AT1R/AKT/β-catenin/Snail signaling pathway in this response.

OUTCOME

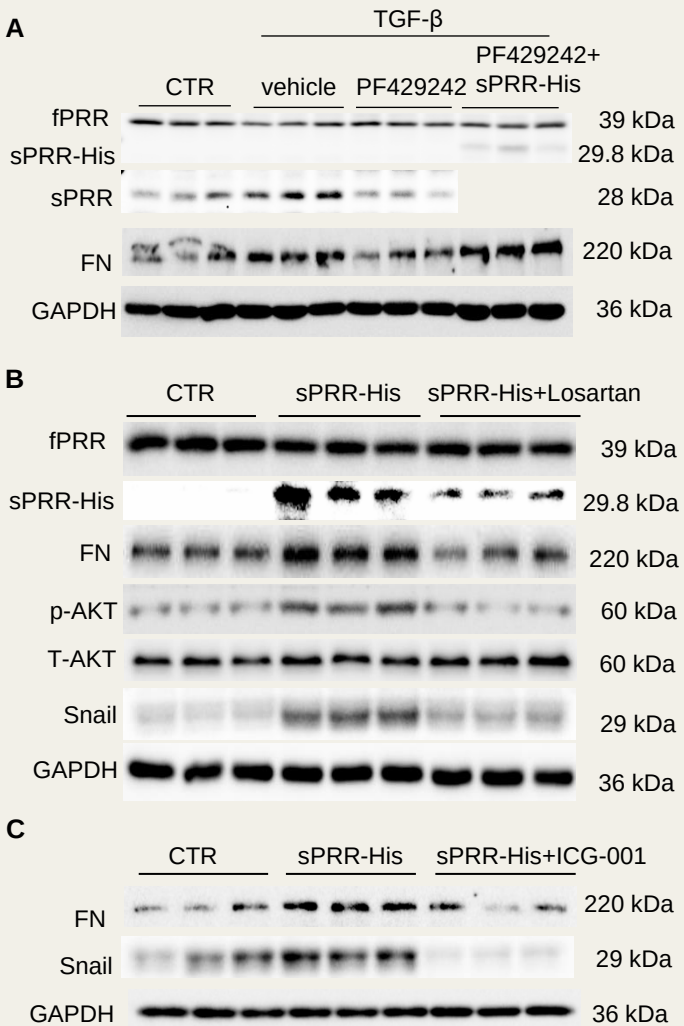

CONCLUSION

1. sPRR contributes to TGF-β induced fibrotic response in HK-2 cells.
2. AT1R/AKT/β-catenin/Snail signaling pathway is responsible for the sPRR-His induced fibrotic response in HK-2 cells.
3. These findings suggest an important role of sPRR in promoting fibrotic response and a potential therapeutic target of chronic renal disease.